Linear Short-Wave Instability in Helical Vortices

Ivan Delbende[1], Yuji Hattori[2], Maurice Rossi[1], Yonghui Xu[1]
[1] Institut Jean le Rond d'Alembert, CNRS, Sorbonne Université
4 Place Jussieu, 75005 Paris, France
[2] Institute of Fluid Science, Tohoku University
2-1-1, Katahira, Aoba-ku, Sendai, Miyagi 980–8577, Japan

ABSTRACT

Due to their peculiar geometry, helical vortices created e.g. in rotor wakes have a non-axisymmetric vortex core. Vortex curvature and ellipticity induce three-dimensional instabilities which are characterized by their wavelength comparable to the core radius. We numerically investigate the growth of such short-wave instabilities linearized in the vicinity of a quasi-steady helical vortex solution, and relate their properties to available asymptotic theories.

1. Introduction

The wake of large size wind turbines and the way it affects the electrical production in a farm need to be accurately predicted. It is however a challenging task because the basic flow structures (tip and root vortices) are not easily characterized. Large-scale flow structures of turbine wakes are often modeled using an array of interlaced helical vortices [1], the temporal instability of which reflects the spatial instability occuring in the real wake. In most cases, the dominant instability involves neighbouring coils, and is referred to as *long-wave instability* [2]. However, helical vortices are also affected by the growth of *short-wave instability* characterized by wavelengths comparable to the vortex core size. The origin of such instability is to be found in the deformation of the vortex core, which can be due to coil-coil interaction, or simply to the curvature of the vortex. Triadic resonances between this steady deformation and a couple of traveling vortex-core waves may then cause so-called curvature [3] and/or elliptic [4] instabilities. In the present paper, we investigate the growth of perturbations in a single quasi-steady helical vortex obtained by direct numerical simulation (DNS) at high Reynolds number. Such instabilities are very sensitive to the vortex parameters, namely helical pitch $2\pi L$ (spatial period of the helix), helical radius R_0, vortex circulation Γ, core size a_0 and axial flow amplitude W_0, which need to be carefully monitored.

2. Methodology

In all the following, polar coordinates (r, θ, z) about the axis z of the helical vortex are used.

2.1 Base Flow

A quasi-steady infinitely long helical vortex solution is first generated, using a dedicated code HELIX [5] which solves the incompressible Navier–Stokes equations in a single plane, with enforced helical symmetry of pitch L. In this formulation, scalar variables and polar components of vector fields depend only on two space variables (r, φ), where $\varphi \equiv \theta - z/L$. The initial condition is a vortex filament with Gaussian helical velocity and vorticity profiles. Such distribution is known to be a quasi-steady state in the limit of infinite pitch, when the vortex is straight. However, this is not the case for helical vortices, which leads to an unsteady transient evolution phase. The procedure detailed in Ref. [6] is here slightly modified to accelerate the convergence towards a quasi-stationary state: a first simulation phase is run at medium Reynolds number ($Re = 3000$) allowing to quickly dampen out transients, then a second phase is run at larger Reynolds number ($Re = 2\pi 10^4$), leading to an approximate base state after a second, relatively short, transient phase. Initial conditions for this double run are then iteratively corrected so as to approach the prescribed parameters in the final state. Here, the reference length and time scales are respectively the radius of the final helical vortex R_0 and the ratio R_0^2/Γ, so that the Reynolds number is defined as $Re = \Gamma/\nu$ (ν is the kinematic viscosity). The nondimensional parameters of the base flow are, beside the unit circulation and helical radius, the following:

- the *reduced helical pitch* $\bar{L} = L/R_0$,
- the nondimensional core size $\bar{a}_0 = a_0/R_0$,
- the *inverse swirl* $\bar{W}_0 = 2\pi W_0 a_0/\Gamma$ that quantifies the amplitude of the axial flow within the vortex core with respect to the aximuthal motion.

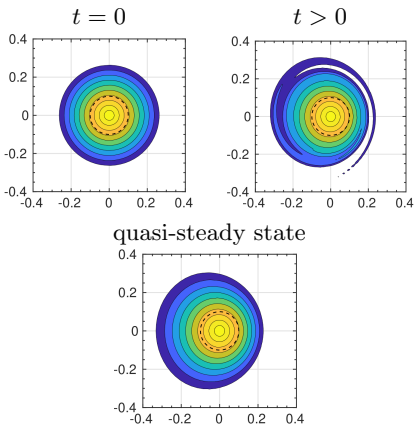

Fig. 1 Example time evolution of a helical vortex with $L = 0.3$. Snapshots of the helical vorticity component represented in a plane orthogonal to its helical centerline.

Corresponding author: Ivan Delbende
E-mail address: ivan.delbende@sorbonne-universite.fr

Table 1 Parameters of the base flows under study.

base flow	$\bar{L}$	$\bar{a}_0$	$\bar{W}_0$
A	0.3	0.11	+0.23
B	0.3	0.11	−0.23
C	0.7	0.15	+0.2
D	0.7	0.15	−0.2

There is no unique way of evaluating the above parameters in a curved vortex: the method used here is described in Ref. [6]. The parameter values for the base flows used in the present study are summarized in table 1. The figure 1 illustrates how the obtained quasi-steady state is not axisymmetric, due to curvature and to interaction with other parts of the helical vortex.

2.2 Instabilities

One of the above high-Reynolds-number, quasi-steady states is then frozen and used as a base flow. Because of helical symmetry, the base pressure as well as base velocity and vorticity polar components only depend on r and φ. Linear perturbations to base quantities can thus be written in the complex framework as a sum of plane waves along z of the form:

$$f(r,\varphi,z,t) = \tilde{f}(r,\varphi)\exp[\mathrm{i}(k_z z - \omega t)]\exp(\sigma t)\,. \quad (1)$$

Here, k_z denotes the real axial wavenumber along z, ω the real frequency of the instability mode and σ its temporal growth rate.

A second dedicated code called HELIKZ is used to determine the dominant instability mode for a fixed arbitrary value of the axial wavenumber k_z. This code indeed solves the Navier–Stokes equations linearized in the vicinity of a helically symmetric base flow, where formula (1) has been injected. The code uses a primitive velocity-pressure formulation, however with complex variables. Details on the code and on the procedure used can be found in Ref. [7].

A first run is performed at some value $k_z^{(0)}$, using divergence-free white noise localized in the core region as an initial condition. The dominant instability mode emerges from the simulation, and its growth rate, frequency and structure can be extracted from simulation results. Such simulation is typically run over more than 100 units of time. Modes on the same branch but with different wavenumbers $k_z^{(n)} = k_z^{(0)} + n\delta k_z$ can be obtained using a simulation at $k_z^{(n)}$ initiated by the final state obtained at $k_z^{(n-1)}$ run over several units of time. This procedure is used to obtain the whole unstable branch.

3. Results

3.1 Elliptic Instability

The first mode studied is obtained through base flow A of table 1, for nondimensional wavenumber $\bar{k}_z \equiv k_z R_0 = 103.3$. This flow is dominated by an instability involving Kelvin waves of azimuthal structures $m = -2$ and $m = 0$, and is called the $(-2, 0, [2, 2])$ elliptical mode [8, 9]. The structure of the (real) helical vorticity perturbation plotted in figure 2 illustrates how such instabities are able to generate small scales within the flow.

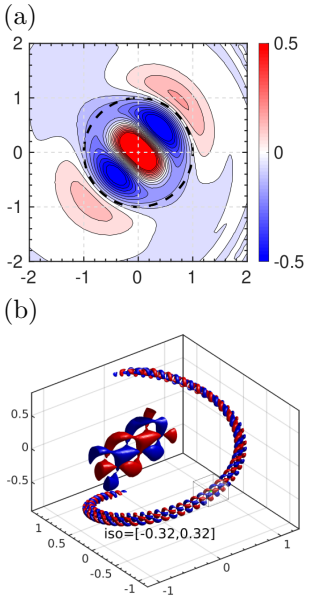

Fig. 2 Perturbation of the helical vorticity for elliptical instability mode $(-2, 0, [2, 2])$ in base flow A for wavenumber $\bar{k}_z = 103.3$ ($\bar{k}_s \approx 3.265$) (a) in a plane locally orthogonal to the helical centerline of the vortex, (b) in 3D over one helix turn.

3.2 Curvature Instability

The second mode investigated is obtained through base flow C of table 1, for wavenumber $\bar{k}_z = 20.3$. This flow is dominated by an instability involving Kelvin waves of azimuthal structures $m = -1$ and $m = 0$, and is called the $(-1, 0, [2, 4])$ curvature mode. Curvature modes have been predicted theoretically in helical vortices [10]. The present study confirms their occurence in a realistic helical vortex for the first time, as revealed in figure 3.

3.3 Comparaison With Theory

Using the procedure described in §2.2, each instability mode may be numerically followed while varying k_z by step, leading to numerically determine growth rate $\sigma(k_z)$ and frequency $\omega(k_z)$. The above results may be compared to those obtained by Blanco–Rodríguez & Le Dizès [9, 10]. These authors have performed an asymptotic theoretical study valid when the core size is much smaller than the radius of curvature or than the helical pitch. The velocity field is expanded in powers of a self-strain parameter

$$\varepsilon = a_0\kappa = \frac{a_0 R_0}{R_0^2 + L^2},$$

where κ is the curvature of the helical vortex. The cases listed in table 1 all have $\varepsilon = 0.1$. In the matched asymptotic expansions, the vortex core structure is at leading order an axisymmetric Batch-

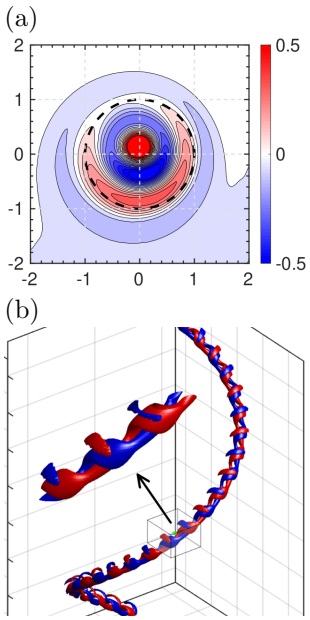

Fig. 3 Same as figure 2 for curvature instability mode $(-1, 0, [2, 4])$ in base flow C for wavenumber $\bar{k}_z = 20.3$ ($\bar{k}_s \approx 1.746$).

elor vortex of core size a_0. Thereafter, small amplitude perturbations around this reference axisymmetric state introduce local effects due to curvature and torsion, and global ones due to the remote vorticity of nearby helix turns that modify this reference structure. Since the z-axis of our helical vortex has no counterpart in the asymptotic theory, we adopt a local nondimensional wavenumber

$$\bar{k}_s = \frac{k_z a_0}{\sqrt{1 + R_0^2/L^2}}$$

defined along the helical centerline, with different space and time reference scales a_0 and $2\pi a_0^2/\Gamma$.

The nondimensional growth rates $\bar{\sigma}$ obtained by DNS and via the asymptotic theory [9] are superimposed in figure 4a, for the elliptic instability of base flows A and B, showing excellent agreement. The only difference between case A and case B is the direction of the axial flow present in the vortex core, such that $\bar{W}_0 = \pm 0.23$. Both flows have the same value of the small parameter ε, which would lead to a unique curve according to Ref. [9], where torsion effects have been overlooked. Restoring torsion effects leads to a differentiation between both cases, as can be seen on the theoretical curves shifted along the $\bar{k}_s$ axis one with respect to the other. This trend is fully confirmed by the DNS results.

Figure 4b shows similar results relative to the growth rate for the curvature mode instability of base flows C and D. Considering the fact that the growth rates are quite small here, the discrepancy between DNS and theory is actually comparable (even smaller!) to that obtained for elliptic instability.

4. Conclusions

Accurate and efficient numerical tools have been designed to study the short-wave instabilities in helical vortices, both of elliptic type and, for the first

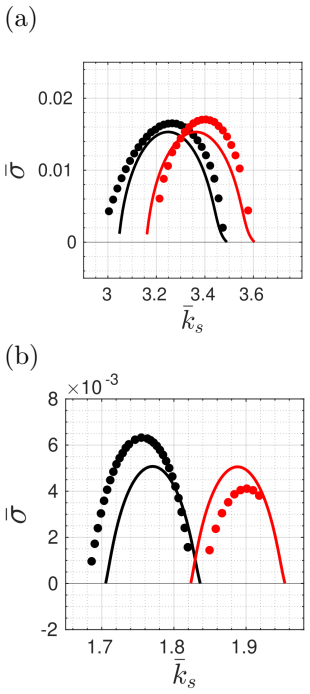

Fig. 4 Growth rate of (a) elliptical instability mode $(-2, 0, [2, 2])$ in base flow A (black) and mode $(0, 2, [2, 2])$ in base flow B (red) and (b) curvature instability mode $(-1, 0, [2, 4])$ in base flow C. Symbols: DNS results. Solid: asymptotic theory.

time, of the curvature type. With respect to recent similar work carried out in the context of vortex rings [11], the instability is found here to be sensitive to the torsion of the basic helical vortex, and thus to the axial flow direction, but presumably also to the helical pitch (investigation in progress).

References

[1] V.L. Okulov, *J. Fluid Mech.*, 521, (2004), 319.

[2] H.U. Quaranta, H. Bolnot, T. Leweke, *J. Fluid Mech.*, 780, (2015), 687.

[3] Y. Hattori, Y. Fukumoto, *Phys. Fluids*, 21(1), (2009), 014104.

[4] R.R. Kerswell, *Annu. Rev. Fluid Mech.*, 34, (2002), 83.

[5] I. Delbende, M. Rossi, O. Daube, *Theoret. Comput. Fluid Dynamics*, 26, (2012), 141.

[6] Y. Xu, I. Delbende, M. Rossi, *J. Fluid Mech.*, 944, (2022), A24.

[7] Y. Xu, *Numerical studies on vortex dynamics: helical vortices and two-phase vortices*, PhD thesis, Sorbonne Université, Paris, France, (2022).

[8] L. Lacaze, K. Ryan, S. Le Dizès, *J. Fluid Mech.*, 577, (2007), 341.

[9] F.J. Blanco-Rodríguez, S. Le Dizès, *J. Fluid Mech.*, 804, (2016), 224.

[10] F.J. Blanco-Rodríguez, S. Le Dizès, *J. Fluid Mech.*, 814, (2017), 397.

[11] Y. Hattori, F.J. Blanco-Rodríguez, S. Le Dizès, *J. Fluid Mech.*, 878, (2019), 5.